Bioorganic & Medicinal Chemistry 16 (2008) 7615–7621

Contents lists available at ScienceDirect

Bioorganic & Medicinal Chemistry

journal homepage: www.elsevier.com/locate/bmc

A concise approach to 1,11-didechloro-6-methyl-4′-*O*-demethyl rebeccamycin and its binding to human serum albumin: Fluorescence spectroscopy and molecular modeling method

Fengling Cui [a,*], Lixia Qin [a], Guisheng Zhang [a,*], Xiaobing Liu [a], Xiaojun Yao [b], Beilei Lei [b]

[a] College of Chemistry and Environmental Sciences, Henan Key Laboratory for Environmental Pollution Control, Henan Normal University, 46 East Construction Road, Xinxiang, Henan 453007, PR China
[b] Department of Chemistry, Lanzhou University, Lanzhou 730000, PR China

ARTICLE INFO

Article history:
Received 31 May 2008
Revised 5 July 2008
Accepted 8 July 2008
Available online 10 July 2008

Keywords:
1,11-Didechloro-6-methyl-4′-*O*-demethyl rebeccamycin
Human serum albumin
Fluorescence quenching
Molecular modeling
Synchronous fluorescence

ABSTRACT

1,11-Didechloro-6-methyl-4′-*O*-demethyl rebeccamycin (JDC-108), a rebeccamycin analog possessing potent anti-tumor activities, was prepared via a concise one-pot strategy in good yield. The interaction between JDC-108 and human serum albumin (HSA) was studied by spectroscopic methods including fluorescence spectroscopy, UV–vis absorption spectrum, and molecular modeling. The quenching mechanism of fluorescence of HSA by JDC-108 was discussed. The number of binding sites n and apparent binding constant *K* were measured by fluorescence quenching method. The thermodynamic parameters ΔH, ΔG, ΔS at different temperatures were calculated and the results indicated the binding reaction was mainly entropy-driven and hydrophobic forces played major role in the reaction. The distance *r* between donor (HSA) and acceptor (JDC-108) was obtained according to Förster theory of non-radiation energy transfer. Synchronous fluorescence and UV–vis absorption spectrum were used to investigate the molecular conformation of HSA molecules with addition of JDC-108 and the result indicated that molecular conformation of HSA molecules was changed in the presence of JDC-108 and the hydrophobic interaction played a major role in JDC-108–HSA association, which was in good agreement with the results of molecular modeling study. In addition, the effect of common ions on the binding constants of JDC-108–HSA complex was also discussed.

1. Introduction

Rebeccamycin and BE-13793C (Fig. 1) were isolated from fermentation cultures of *Saccharotrix aerocolonigenes* (*ATCC* 39243)[1] and *Streptoverticillium mobaraense* (*FERM P*-10489).[2] Their structures share a common indolocarbazole pharmacophore. Since the potent anti-cancer activities were discovered for these compounds, the indolocarbazole compounds have been extensively studied. Structure–activity relationship studies have led to the development of several analogs. Recently, Zhang et al. reported a rebeccamycin analog, 1,11-didechloro-6-methyl-4′-*O*-demethyl rebeccamycin (JDC-108, Fig. 1), that displayed similar activity to the parent compound rebeccamycin (IC_{50} 4–6 μM) in two cancer cell lines, including colorectal carcinoma cells (SW620) and leukemia cells (K562) and strong topoisomerase inhibition in vivo complex of topoisomerase (ICT) bioassay in HeLa cells.[3] Compared with rebeccamycin, JDC-108 is easier to synthesize, with a simple structure without chlorine atoms at the C1, C11 positions and methyl group at 4′-O position of sugar moiety. It is worthy of further evaluation as a new drug candidate.

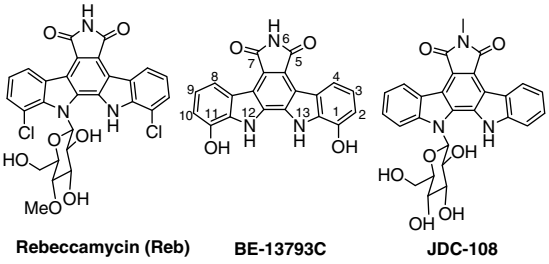

Figure 1. Structures of rebeccamycin and its analogs.

Human serum albumin (HSA) is the most abundant protein in the circulatory system. Its principal function is to transport fatty acids, while it is also capable of binding an extraordinarily broad range of drugs.[4] Much of the clinical and pharmaceutical interest in the protein derives from its effects in drug pharmacokinetics.[5]

* Corresponding authors. Tel./fax: +86 373 3326336 (F.L.C.); tel./fax: +86 10 3325250 (G.S.Z.).
E-mail addresses: fenglingcui@hotmail.com (F. Cui), zgs6668@yahoo.com (G. Zhang).

0968-0896/$ - see front matter © 2008 Elsevier Ltd. All rights reserved.
doi:10.1016/j.bmc.2008.07.017

The crystallographic analysis of HSA revealed that the protein, a 585-amino acid residue monomer, contains three homologous-helical domains (I–III) and a single tryptophan (Trp214).[6] HSA can bind and carry through the bloodstream many drugs, which are poorly soluble in water. It has been shown that the distribution, free concentration, and the metabolism of various drugs can be significantly altered as a result of their binding to HSA.[7] Drug interactions at protein binding level will in most cases significantly affect the apparent distribution volume of the drugs and also affect the elimination rate of drugs; therefore, the studies on this aspect can provide information of the structural features that determine the therapeutic effectivity of drugs and that have been an interesting research field in life sciences, chemistry, and clinical medicine.

Many drugs and other bioactive small molecules bind reversibly to albumin and other serum components,[8–10] which implicates HSA's role as carriers. Serum albumin often increases the apparent solubility of hydrophobic drugs in plasma and modulates their delivery to cells in vivo; they can play a dominant role in drug disposition and efficacy.[11] Accordingly, it is important to understand and predict ligand/drug displacement interactions for a variety of endogenous and exogenous ligands/drugs. However, the detailed investigation on the binding interaction of HSA and JDC-108 has not been reported. Fluorescence spectroscopy is a powerful tool for the study of the reactivity of chemical and biological systems. For fluorescence quenching, the decrease in intensity is described by the well-known Stern–Volmer equation ($F_0/F = 1 + K_{SV}[Q]$).[12] The aim of our work was to determine the affinity of JDC-108 to HSA and to investigate the thermodynamics of their interaction. We also tried to find the stoichiometry of JDC-108 and HSA binding. In order to attain these objectives, we planned to carry out detailed investigation of JDC-108–HSA association using fluorescence spectroscopy and UV–vis absorbance spectroscopy. Through fluorescence resonance energy transfer (FRET) and synchronous fluorescence spectra, we planned to further investigate the effect of energy transfer and the effect of JDC-108 binding on the environment adjacent to the tryptophan residue in HSA.

2. Materials and methods

2.1. The preparation of JDC-108

JDC-108 was prepared via a one-pot procedure (Scheme 1): 2,3-Bis-(1H-indol-3-yl)-*N*-methylmaleimide **1** (100.0 mg, 0.29 mmol) was added to cold (0 °C) TFA (2.5 mL) with stirring in a 10 mL flask. The resulting dark red solution was stirred under N_2 at 0 °C for 8 h until the reaction was complete. Cold (0 °C) hexane (2 mL) was added slowly and the layers were separated. Hexane and TFA were removed in vacuo. The red crude was diluted in EtOAc (10 mL) and washed with satd. $NaHCO_3$ solution (3 × 10 mL) and then brine (3 × 10 mL), dried ($MgSO_4$), filtered, and concentrated to afford intermediates **2** as a red-orange solid, which was allowed to be used in the next step reaction without further purification.

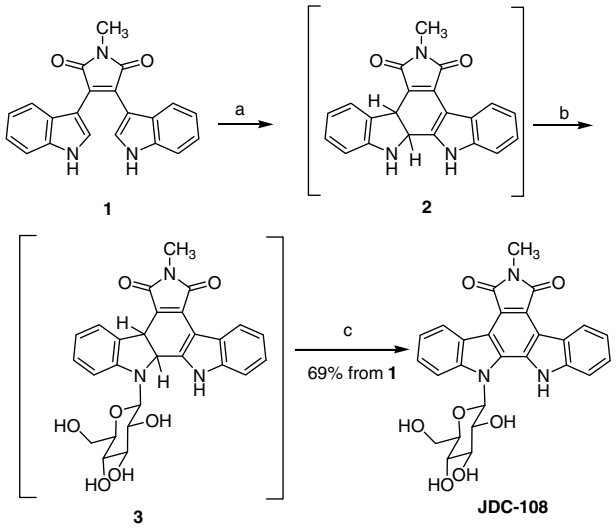

Scheme 1. Reagents and conditions: (a) CF_3CO_2H, 0 °C, 8 h; (b) $(NH_4)_2SO_4$, glucose, 90 °C, 6h; (c) DDQ, rt, overnight.

In a flask of 100 mL, indole-indoline **2** obtained above, anhydrous D-glucose (261.2 mg, 1.45 mmol), and $(NH_4)_2SO_4$ (115.0 mg, 0.87 mmol) were combined with EtOH (30 mL) and heated to reflux at 90 °C for 6 h. After reaction completion, the solvent was removed in vacuo. The crude mixture was dissolved in THF (30 mL), and DDQ (72.4 mg, 0.32 mmol) was added. The reaction mixture was stirred at room temperature overnight, then quenched with saturated $NaHCO_3$ solution (10 mL), diluted with EtOAc, and the layers were separated. The organic layer was extracted with saturated $NaHCO_3$ (3 × 10 mL) and washed with brine (3 × 10 mL), dried over $MgSO_4$, filtered, and concentrated onto silica gel. Purification by silica gel chromatography (CH_2Cl_2/CH_3OH = 50:1) yielded JDC-108 (101.2 mg, 69% from **1**): ^{1}H NMR (400 MHz, DMSO-d_6) δ 3.20 (s, 3H), 3.52–3.58 (m, 2H), 3.80 (d, 1H, J = 10.8 Hz), 3.93–4.02 (m, 2H), 4.05–4.08 (m, 1H), 4.91 (d, 1H, J = 5.2 Hz), 5.12 (d, 1H, J = 5.2 Hz), 5.38 (d, 1H, J = 4.8 Hz), 5.99 (d, 1H, J = 3.6 Hz), 6.27 (d, J = 8.4 Hz, 1H, *H*-1′), 7.34–7.39 (m, 2H), 7.53–7.60 (m, 2H), 7.68 (d, 1H, J = 8.0 Hz), 7.96 (d, 1H, J = 8.8 Hz), 9.09 (d, 1H, J = 8.0 Hz), 9.16 (d, 1H, J = 8.0 Hz), 11.65 (s, 1H).

2.2. Materials

Appropriate amounts of human serum albumin (Hualan Biological Engineering Limited Company) were directly dissolved in water to prepare stock solution at final concentration of 2.0×10^{-5} M and stored in the dark at 0–4 °C. 7.20×10^{-5} M JDC-108, 0.5 M NaCl working solution, 0.1 M Tris–HCl buffer solution of pH 7.4 and other ionic solutions were prepared. All chemicals were of analytical reagent grade and were used without further purification. Double distilled water was used throughout.

2.3. Apparatus

All fluorescence spectra were recorded on an FP-6200 spectrofluorimeter (JASCO, Japan) and a RF-540 spectrofluorimeter (Shimadzu, Japan) equipped with a thermostat bath, using 5 nm/5 nm slit widths. The UV absorption spectra were performed on a Tu-1810 UV–vis spectrophotometer (Beijing General Instrument, China). The pH values were measured on a pH 3 digital pH-meter (Shanghai Lei Ci Device Works, Shanghai, China) with a combined glass electrode. All calculations were performed on SGI workstation while studying the molecular model.

2.4. Measurements of spectrum

Under the optimum physiological conditions described above, 2.0 mL Tris–HCl buffer solution, 2.0 mL NaCl solution, appropriate amounts of HSA and JDC-108 were added to 10.0 mL volumetric flask and diluted to 10.0 mL with double distilled water. Fluorescence quenching spectra of HSA were obtained at excitation wavelength (280 nm) and emission wavelength (300–450 nm). Fluorescence spectra in the presence of other ions were also measured at the same conditions. In addition, the UV absorption and synchronous fluorescence spectra of system were recorded.

2.5. Characteristics of synchronous fluorescence method

The synchronous fluorescence spectra were obtained by simultaneously scanning the excitation and emission monochromators. Thus, the synchronous fluorescence applied to the equation of synchronous luminescence[13]

$$F = kcdE_{ex}(\lambda_{em} - \Delta\lambda)E_{em}(\lambda_{em}) \quad (1)$$

where F is the relative intensity of synchronous fluorescence, $\Delta\lambda = \Delta\lambda_{em} - \lambda_{ex}$ is a constant, E_{ex} is the excitation function at the given excitation wavelength, E_{em} is the normal emission function at the corresponding emission wavelength, c is the analytical concentration, d is the thickness of the sample cell, and k is the characteristic constant comprising the 'instrumental geometry factor' and related parameters. Since the relationship of the synchronous fluorescence intensity (F) and the concentration of JDC-108 should follow the F equation, F should be in direct proportion to the concentration of JDC-108.

The optimal values of the wavelength intervals ($\Delta\lambda$) are important for the correct analysis and interpretation of the binding mechanism. When the wavelength interval ($\Delta\lambda$) was fixed at 60 nm of protein, the synchronous fluorescence had the same intensity as the emission fluorescence following excitation at 280 nm, just the maximum emission wavelength and shape of the peaks were changed.[14–16] Thus, the synchronous fluorescence measurements can be applied to calculate association constants similar to the emission fluorescence measurements. Therefore, the synchronous fluorescence measurements can deduce the binding mechanism as the emission fluorescence measurements did. In this study, the synchronous fluorescence spectra of tyrosine residues and tryptophan residues were measured at $\lambda_{em} = 280$ nm ($\Delta\lambda = 15$ and 60 nm) in the absence and presence of various amounts of JDC-108.

2.6. Protein–ligand docking study

The potential of the 3D structures of HSA was assigned according to the Amber 4.0 force field with Kollman-all-atom charges. The initial structures of all the molecules were generated by molecular modeling software Sybyl 6.9.1. The geometries of this drug were subsequently optimized using the Tripos force field with Gasteiger–Marsili charges. The AutoDock3.05 program was used to calculate the interaction modes between the drug and HSA. Lamarckian genetic algorithm (LGA) implemented in Autodock was applied to calculate the possible conformation of the drug that binds to the protein. During docking process, a maximum of 10 conformers was considered for the drug. The conformer with the lowest binding free energy was used for further analysis. All calculations were performed on SGI FUEL workstation.

3. Results and discussion

3.1. Chemistry

In our previous work, the compound JDC-108 was successfully synthesized from bisindolylmaleimide **1** bearing a methyl group at the imide nitrogen via a multistep strategy which is outlined in Scheme 2.[3] The coupling reaction of indolylmagnesium bromide with *N*-methyldichloromaleimide provided the bisindolylmaleimide intermediate **1**. Compound **4** was prepared via oxidative photocyclization of **1**. N-glycosylation of compound **4** with tetra-*O*-benzyl glucopyranosyl chloride, which was prepared from glucose through three reaction steps, was performed in the presence of potassium hydroxide and the hydrogenation debenzylation led to compound JDC-108. This approach required six reaction steps including full protection of the carbohydrate hydroxyl groups. Of all procedures for glycosylation of indoles and indolocarbazoles Faul's method is an important strategy because selective glycosylation can be achieved using unprotected, unactivated carbohydrates.[17] Faul's method is an efficient two-step process to prepare indolo[2,3-*a*]carbazole glycoside analogs of rebeccamycin. The substrate of Faul's method is similar to **1**, only difference between them is a methyl group at the imide nitrogen of compound **1**, which allowed us to follow Faul's method to prepare JDC-108. Using conditions similar to those developed by Faul group, however, the corresponding intermediate **2** (Scheme 1) was not obtained in pure due to its unstability. Fortunately, the intermediate **2** remained intact during work-up, which allowed us to develop a one-pot procedure, in which the crude **2** was used directly in glycosylation step without purification and the glycosylated indole-indoline **3** was also used directly in oxidation step without isolation (Scheme 1). After the cyclization reaction was complete, the crude **2** was washed and concentrated to dryness, and excess D-glucose and ammonium sulfate in EtOH was added. Once the glycosylation was complete, the solvent was removed in vacuo. The crude mixture was dissolved in THF, and DDQ was added. After oxidation, the desired pure compound JDC-108 was isolated in 69% yield from **1** (Scheme 1). This one-pot approach to JDC-108 was very effective and concise.

3.2. Biology

3.2.1. Fluorescence quenching studies of HSA by JDC-108

Fluorescence intensity of a compound can be decreased by a variety of molecular interactions, viz., excited-state reactions, molecular rearrangements, energy transfer, ground state complex formation, and collisional quenching. Studying this quenching process can give some information of the binding of small molecule substances to protein, such as the binding mechanism, binding mode, binding constants, binding sites and intermolecular distances.

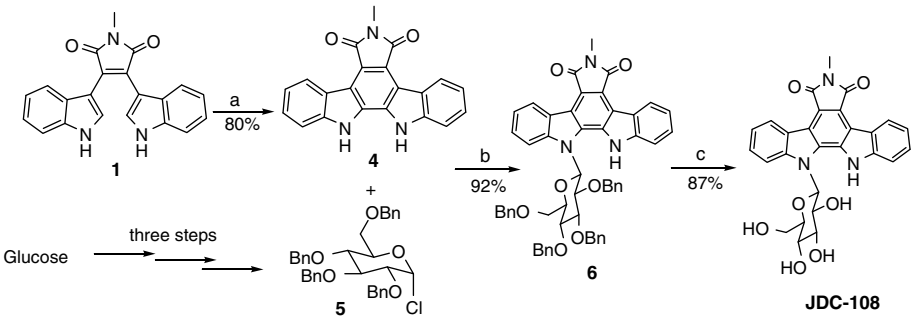

Scheme 2. Reagents and conditions: (a) *hv*, air, I_2, THF/MeCN, 15 h; (b) NaOH, Na_2SO_4, MeCN, rt, 24 h; (c) Pd/C, H_2 45 psi, 10 h.

An intrinsic fluorescence experiment was performed to evaluate the interaction of JDC-108 to HSA. The effect of JDC-108 on the HSA fluorescence spectra is shown in Figure 2. The fluorescence intensity of HSA gradually decreased upon increasing the concentration of JDC-108, indicating the binding of JDC-108 to HSA. The maximum wavelength of HSA shifted from 340 to 349 nm after the addition of JDC-108. Under the same condition, no fluorescence of JDC-108 was observed. Therefore, the observed spectral shift should be due to the conformational changes induced by the interaction leading to a further exposure of tryptophan residue to the polar solvent.[18] This spectral shift also indicated that the binding site of JDC-108 on HSA was very close to the tryptophan residue.

The fluorescence quenching behavior is known to occur mainly by a collisional process and/or formation of a complex between quencher and fluorophore.[19] There is no fluorescence emission from JDC-108 at the range of 300–450 nm, thus the contribution of the JDC-108 could be neglected when measuring the protein fluorescence emission spectra at different JDC-108 concentrations. Regression curve was plotted according to Stern–Volmer equation (Eq. (1))[20,21] for fluorescence quenching of HSA induced by JDC-108 is shown in Figure 3:

$$F_0/F - 1 = K_{SV}[Q] = k_q\tau_0[Q] \quad (2)$$

where F and F_0 are the fluorescence intensity of HSA in the presence and absence of quencher, [Q] the quencher concentration and K_{SV} the Stern–Volmer quenching constant, which is the product of the bimolecular quenching constant (k_q) and life time of the fluorophore in the absence of quencher (τ_0).

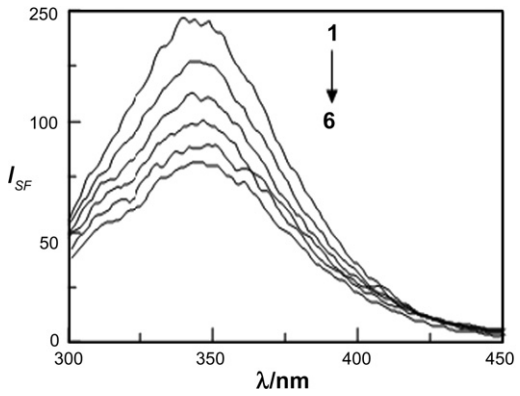

Figure 2. The fluorescence spectra of JDC-108–HSA system. From 1 to 6: $C_{HSA} = 2.0 \times 10^{-5}$ M; $C_{JDC\text{-}108} = 0, 7.2, 14.4, 21.6, 28.8, 36 \times 10^{-7}$ M.

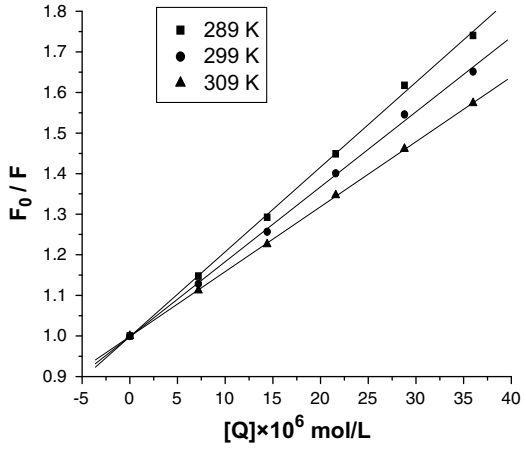

Figure 3. The Stern–Volmer curves for quenching of JDC-108 with HSA.

Table 1
The dynamic quenching constants (L/(mol s)) between JDC-108 and HSA

T (K)	Stern–Volmer equation	k_q (L/(mol s)	R
289	$Y = 0.9983 + 2.09 \times 10^5[Q]$	2.09×10^{13}	0.9994
299	$Y = 0.9983 + 1.85 \times 10^5[Q]$	1.85×10^{13}	0.9993
309	$Y = 0.9984 + 1.60 \times 10^5[Q]$	1.60×10^{13}	0.9999

The linear regression equation, $F_0/F = 20{,}900[Q] + 0.9983$ ($R = 0.9994$), suggests that the quenching behavior in the present system could be interpreted by the Stern–Volmer equation. The Stern–Volmer quenching constant K_{SV} was obtained by the slope of regression curves and the bimolecular quenching constant (k_q) was calculated (as to Ref. 18, τ_0 is about 10^{-8} s), and is listed in Table 1. Since the bimolecular quenching constants (k_q), which was deduced from K_{SV} and τ_0, are larger than the limiting diffusion rate constant of the biomolecule (2.0×10^{10} L/(mol s)),[22,23] the static quenching could be the main mechanism of the fluorescence quenching of HSA by JDC-108.

3.2.2. Binding constants

In drug–protein binding studies, several equations have been used for binding constant calculation. One frequently used is Scatchard equation[24]

$$r/D_f = nK - rK \quad (3)$$

where r is the number of mol of bound drug per mol of protein, D_f is the concentration of unbound drug, K is the binding constant, and n is the number of binding sites. Figure 4 shows the Scatchard plots for the JDC-108–HSA system at different temperatures. The linearity of the Scatchard plot indicated that JDC-108 bound to a single class of binding sites on HSA, which was full agreement with the number of binding site n; and the binding constants (K, Table 2) agree very closely with those obtained by the modified Stern–Volmer equation. In addition, it was found that there was a strong interaction between JDC-108 and HSA, and the binding constant decreased with the increasing temperature, resulting in a reduction of the stability of the JDC-108–HSA complex, but the effect of temperature is very small. Thus, the quenching efficiency of JDC-108 to HSA is not reduced significantly within a small temperature range. In this work, the binding constants obtained with the modified Stern–Volmer equation are applied in the discussion of binding modes.

3.2.3. Binding mode

Generally, small molecules are bound to macromolecules through four binding modes: hydrogen bond, van der Waals force, electrostatic and hydrophobic interactions, etc.[25]

The thermodynamic parameters, enthalpy (ΔH) and entropy (ΔS) of reaction are important for confirming the acting force.

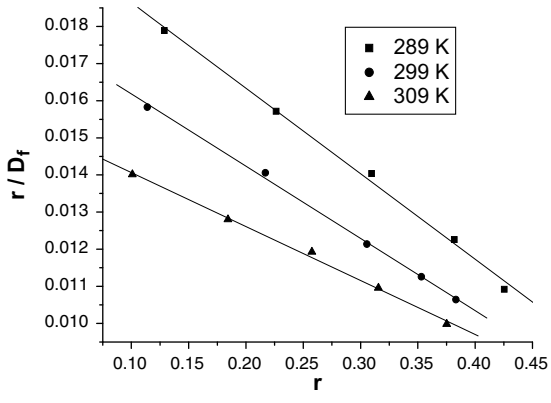

Figure 4. Scatchard plot for the JDC-108–HSA.

Table 2
The binding constant (K, M) between JDC-108 and HSA

T (K)	Scatchard equation	K (L/mol)	n	R
289	$Y = 0.0230 - 0.0231r$	2.31×10^5	0.9957	0.9980
299	$Y = 0.0182 - 0.0195r$	1.95×10^5	0.9333	0.9991
309	$Y = 0.0155 - 0.0145r$	1.45×10^5	1.0689	0.9983

For this reason, the temperature dependence of the binding constant was studied. Temperatures 289, 299, and 309 K were chosen to avoid HSA structural degradation. The thermodynamic parameters can be determined from the van't Hoff equation

$$\ln K = -\Delta H/RT + \Delta S/R \quad (4)$$

K is the binding constant at temperature T and R is gas constant. The values of ΔH and ΔS were obtained from linear van't Hoff plot and are presented in Table 3. The value of ΔG as calculated from the relation

$$\Delta G = \Delta H - T\Delta S \quad (5)$$

Many references have reported the characteristic sign of the thermodynamic parameter associated with the various individual kinds of interaction that may take place in the protein association process.[26,27] From the point of view of water structure, a positive ΔS value is frequently taken as evidence for hydrophobic interaction. Moreover, specific electrostatic interactions between ionic species in aqueous solution are characterized by a positive ΔS value and a negative ΔH value. As shown in Figure 5, JDC-108 carries a positive charge in aqueous solution. The binding of JDC-108 to HSA might involve electrostatic interactions. Accordingly, it is not possible to account for the thermodynamic parameters of JDC-108–HSA complex on the basis of a single intermolecular force model. It is more likely that hydrophobic, electrostatic interactions are involved in its binding process.

3.2.4. Binding distance

There is a good overlapping between the fluorescence emission spectrum of free HSA and absorption UV spectra of the drug

Table 3
The thermodynamic parameters for the JDC-108 binding to HSA

T (K)	ΔG (kJ/mol)	ΔH (kJ/mol)	ΔS (J/(mol K))
289	−29.67		
299	−30.28	−12.17	60.56
309	−30.53		

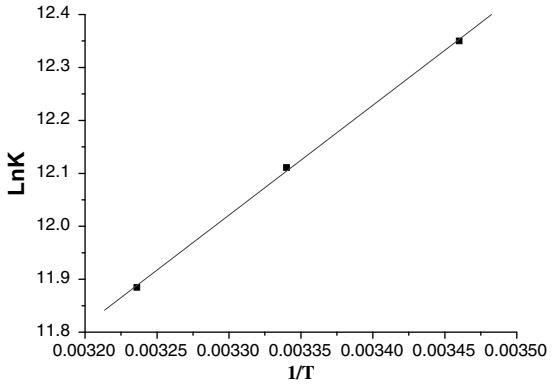

Figure 5. Van't Hoff plot for the interaction of JDC-108 and HSA.

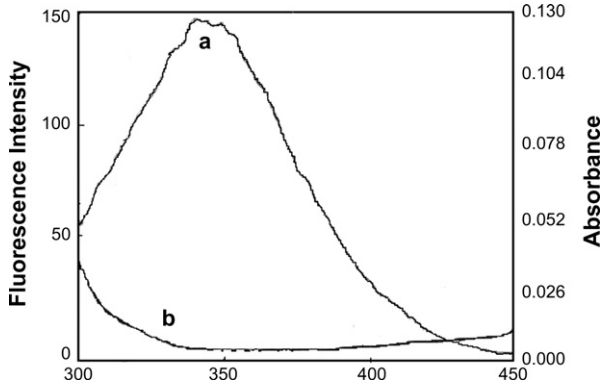

Figure 6. The overlap of UV absorption spectrum of JDC-108 with the fluorescence emission spectrum of HSA. (a) The fluorescence emission spectrum of HSA (8×10^{-7} M); (b) the UV absorption spectrum of JDC-108 (7.20×10^{-7} M).

(Fig. 6). As the fluorescence emission of protein was affected by the excitation light around 280 nm, the spectrum ranging from 300 to 450 nm was chosen to calculate the overlapping integral. According to Förster's theory,[28,29] the energy transfer efficiency E is defined as the following equation,

$$E = R_0^6/(R_0^6 + r^6) \quad (6)$$

where r is the distance from the ligand to the tryptophan amino acid residue of the protein and R_0 is the Förster critical distance, at which 50% of the excitation energy is transferred to the acceptor. It can be calculated from donor emission and acceptor absorption spectra using the Förster formula,

$$R_0^6 = 8.8 \times 10^{-25} k^2 n^{-4} \Phi J \quad (7)$$

where K^2 is a factor that describes the relative orientations of the donor and acceptor, Φ is the fluorescence quantum yield of donor in the absence of acceptor; n is the refractive index of the medium between the donor and acceptor. Given that the fluorescence quantum yield Φ of tryptophan is 0.118, the refractive index n of the medium is the average value of water and organic solute (1.366) and K^2 is 2/3 for random orientation,[30] J is the integral that defines the amount of overlapping areas between the normalized fluorescence emission spectrum of the donor and the UV absorption spectrum of the acceptor and was calculated by dividing the area of the overlapped region.

$$J = \sum F(\lambda)\epsilon(\lambda)\lambda^4 \Delta\lambda / \sum F(\lambda)\Delta\lambda \quad (8)$$

$F(\lambda)$ is the fluorescence intensity of donor in the absence of the acceptor at wavelength λ and $\varepsilon(\lambda)$ is the UV molar absorption coefficient of the acceptor at λ.

E can be estimated from the following formula:

$$E = 1 - F/F_0 \quad (9)$$

where F_0 and F is the fluorescence intensity of donor in the absence and presence of equal amount of acceptor, respectively. If the value of E, K^2, Φ and n is known, R_0 and r can be calculated.

The calculated results showed that R_0 for JDC-108 was 2.34 and the binding distance r was 3.22, respectively. There is only one tryptophan residue in HSA, Trp214, and the distance from the bound ligands to Trp214 is less than 7 nm, which suggested that a non-radioactive energy transfer mechanism may be among the quenching mechanisms.[21,31] While the binding distance r of the drugs was more than their respective critical distance R_0, the fluorescence quenching was more likely induced by static quenching other than non-radioactive energy transferring.[21,31]

3.2.5. Molecular modeling

The complementary application of molecular modeling by computer methods has been employed to improve the understanding of the interaction between JDC-108 and HSA. Descriptions of 3D structure of crystalline albumin have revealed that HSA comprises of three homologous domains (I–III): I (residues 1–195), II (196–383), III (384–585), each domain is a product of subdomains that posses common structural motifs. The principal regions of ligand binding to HSA are located in hydrophobic cavities in subdomains IIA and IIIA, which are consistent with sites I and II, respectively. One tryptophan residue (Trp214) of HSA is in subdomain IIA.[32] The crystal structure of HSA was taken from the Brookhaven Protein Data Bank (entry codes 1h9z). The potential of the 3D structure of HSA was assigned according to the Amber 4.0 force field with Kollman-all-atom charges. The initial structure of all the molecules was generated by molecular modeling software Sybyl 6.9. The geometries of these compounds were subsequently optimized using the Tripos force field with Gasteiger–Marsili charges. FlexX program was applied to calculate the possible conformation of the ligands that binds to the protein. The conformer with RMS (root-means-square) was used for further analysis. Based on this kind of approach, a computational model of the target receptor has been built, by which partial binding parameters of the JDC-108–HSA system were calculated through SGI FUEL workstations. The best energy ranked results are shown in Figure 7, on which the bisindolylmaleimide moiety is located within the binding pocket and both rings are practically coplanar. It is important to note that the tryptophan residue (Trp214) and the lysine residue (Lys195) of HSA are in close proximity to the pentenyl moiety of JDC-108, suggesting the existence of hydrophobic interaction between them. Further, this finding provides a good structural basis to explain the efficient fluorescence quenching of HSA emission in the presence of JDC-108. There are also hydrogen bonds between the drug and the polar amino acid residues: Arg218, Arg222, His242, and Ala291 from the IIA subdomain are able to form intermolecular H-bond with ring. On the other hand, the amino acid residues with benzene ring can match that of the structure of JDC-108 in space in order to firm the conformation of the complex. The ligand binding regions of HSA located in hydrophobic cavities in subdomains IIA are large to accommodate the JDC-108. The calculated binding Gibbs free energy (ΔG) is -21.4 kJ mol^{-1}, which was not close to the experimental data (-29.67 kJ mol^{-1}) in some degree. However, the results obtained from modeling indicated that the interaction between JDC-108 and HSA was dominated by hydrophobic force.

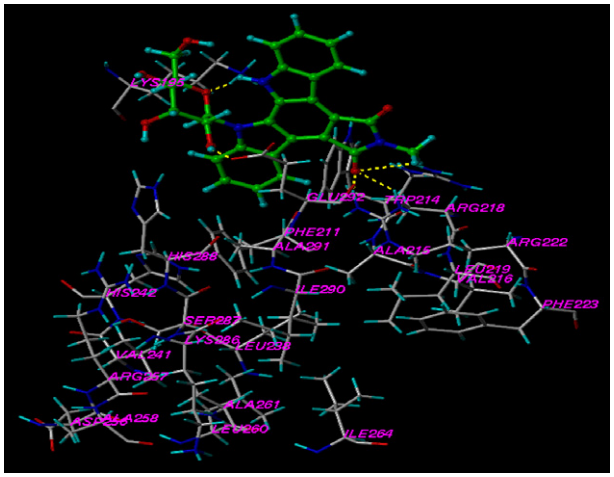

Figure 7. The interaction model between JDC-108 and HSA. The residues of JDC-108 and HSA are represented using different tinctorial stick model. The hydrogen bond between the ligand and the protein is indicated by dashed line.

3.2.6. Conformation investigation

Spectroscopy is an ideal tool to observe conformational changes in proteins since it allows non-intrusive measurements of substances in low concentration under physiological conditions. It is advantageous to use intrinsic fluorophores for these investigations in order to avoid complicated labeling with an extrinsic dye. Tryptophan is highly sensitive to the local environment and also displays a substantial spectral shift. As a result, the position of the spectra maximum (λ_{max}) depends on the properties of the environment of the tryptophan residues,[33] and the fluorescence spectra depends upon the degree of exposure of the tryptophan side chain to the polar, aqueous solvent and upon its proximity to specific quenching groups.[34] Hence, it could be used as an ideal tool to study protein structure and conformation.

For reconfirming the structural change of HSA by addition of JDC-108, we measured the UV–vis absorbance spectra of HSA (Fig. 8) and synchronous fluorescence spectra (Fig. 9) of HSA with various amounts of JDC-108. Figure 8 displays the UV–vis absorbance spectra of HSA at different contents of JDC-108. It is clear from the figure that the baselines of the UV–vis absorbance spectra at 340–300 nm are raised and the maximum absorption spectra blue shift (from 323 to 319 nm), indicating that the HSA molecules associate with JDC-108 to form a JDC-108–HSA complex and the peptide strand extended even more, while the hydrophobicity was decreased (or became more polar). The conclusion agrees with the result of conformational changes by synchronous fluorescence spectra, which indicates that the approach of synchronous fluorescence spectroscopy is scientific.

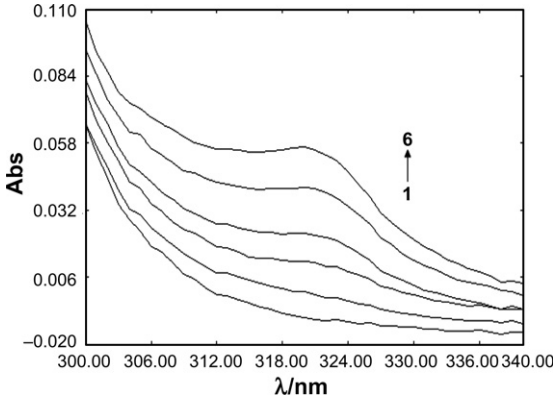

Figure 8. UV absorption spectra of HSA in the absence and presence of JDC-108 (1) The UV absorption of HSA, $C_{HSA} = 8 \times 10^{-7}$ M. (2) The UV absorption of JDC-108, $C_{JDC\text{-}108} = 4.07 \times 10^{-6}$ M. (3–6) The UV absorption of JDC-108–HSA, $C_{HSA} = 8 \times 10^{-7}$ M; $C_{JDC\text{-}108} = 7.20 \times 10^{-7}$ M, $C_{JDC\text{-}108} = 14.4 \times 10^{-7}$ M, $C_{JDC\text{-}108} = 21.6 \times 10^{-7}$ M, $C_{JDC\text{-}108} = 28.8 \times 10^{-7}$ M.

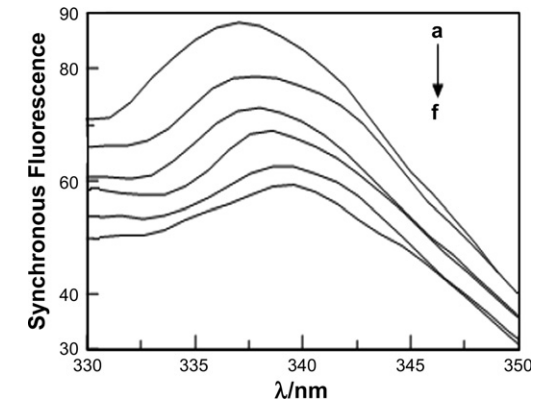

Figure 9. Synchronous fluorescence spectrum of HSA ($T = 289$ K, pH 7.40), $C_{HSA} = 2 \times 10^{-5}$ M, $C_{JDC\text{-}108}/(10^{-7}$ M), (a)–(f) 0, 7.20, 14.4, 21.6, 28.8, 36.

Table 4
The binding constants between JDC-108 and HSA in the presence of other ions

Ions	K ($\times 10^6$)	R	Ions	K	R
Ca^{2+}	7.17	0.9992	Ni^{2+}	5.32	0.9998
Fe^{3+}	3.48	0.9991	Cd^{2+}	4.56	0.9997
F^-	8.78	0.9985	Bi^{3+}	7.01	0.9994
SiO_3^{2-}	6.68	0.9986	Zn^{2+}	7.12	0.9990
Pb^{2+}	4.87	0.9997	K^+	8.90	0.9998
CO_3^{2-}	3.48	0.9995	Al^{3+}	3.93	0.9996
Mg^{2+}	4.76	0.9988	Hg^{2+}	8.41	0.9991
SO_4^{2-}	4.33	0.9995	NO_3^-	3.40	0.9997

Synchronous fluorescence spectroscopy introduced by Llody[35,36] has been used to characterize complex mixtures providing fingerprints of complex samples.[37] It involves the simultaneous scanning of excitation and the fluorescence monochromators of a fluorimeter, while maintaining a fixed wavelength difference ($\Delta\lambda$) between them. The synchronous fluorescence spectra give information about the molecular environment in a vicinity of the chromospheres molecules. In the synchronous spectra, the sensitivity associated with fluorescence is maintained while offering several advantages: spectral simplification, spectral bandwidth reduction and avoiding different perturbing effects. The authors[38] suggested a useful method to study the environment of amino acid residues which was by measuring the possible shift in maximum emission wavelength λ_{max}, the shift in position of maximum emission corresponding to the changes of the polarity around the chromophore molecule. When the λ-value ($\Delta\lambda$) between excitation wavelength and emission wavelength was stabilized at 60 nm, the synchronous fluorescence gives the characteristic information of tryptophan residues.[39] The effect of JDC-108 on HSA synchronous fluorescence spectroscopy is shown in Figure 9.

It is apparent from Figure 9 that the maximum emission wavelength red shift (from 336 to 340 nm) at the investigated concentration range when $\Delta\lambda = 60$ nm. The red shift of the maximum emission suggests a more polar (or less hydrophobic) environment of the Trp214 residue. The conclusion agrees with the result of conformational changes by UV–vis absorbance spectra.

3.2.7. The effect of common ions on the binding constant

The effect of common ions viz., SO_4^{2-}, F^-, NO_3^-, Mg^{2+}, Cd^{2+}, K^+ and Ca^{2+} on the binding of JDC-108 to HSA was investigated at 289 K by recording the fluorescence intensity of JDC-108–HSA complex in the presence of each ion, separately in the range of 300–450 nm upon excitation at 280 nm. Under the experimental conditions, no cation gave precipitate in phosphate buffer. The effects of such cations on binding of a drug to HSA have also been reported in the literature.[28] The fluorescence emission spectrum of JDC-108 in the presence of common ion shows that there is no interaction between the common ion and JDC-108. But, there is a binding reaction between the common ion and protein and thus the presence of common ion directly affects the binding between JDC-108 and HSA. As evident from Table 4, the presence of common ions reduced the JDC-108–HSA binding constant. As a result, the binding force between protein and drug also increased and prolonged the stored time of drug in blood plasma. This may lead to the need for more doses of JDC-108 to achieve the desired therapeutic effect.

4. Conclusions

An effective one-pot approach to JDC-108 has been developed. The interaction between JDC-108 and HSA was studied by fluorescence spectroscopy combined with UV–vis, molecular modeling and synchronous fluorescence spectrophotometric techniques under simulative physiological conditions for the first time. This study showed that the intrinsic fluorescence of HSA was quenched through static quenching mechanism and JDC-108 most likely bound to the hydrophobic pocket located in subdomain IIA. Experimental results also showed that the binding of JDC-108 to HSA induced a conformational change of HSA, which was further proved by the quantitative analysis data of UV–vis and synchronous fluorescence spectra. In addition, we inferred that the binding force was mainly hydrophobic interaction; two other interactions, electrostatic attraction and hydrogen bond were also involved in the binding process. We hope this work will be used as a useful guideline for efficient indolocarbazole drug design.

Acknowledgments

This work was sponsored by the Nature Science Foundation of China (No. 20673034), the Young Backbone Teacher Sustentation Plan of Henan Universities (No. 200470) and Department of Education of Henan Province (No. 2006150012) to F.C; National Natural Science Foundation of China (20672031), the Program for New Century Excellent Talents in University of Henan Province (2006-HACET-06), and Innovation Scientists and Technicians Troop Construction Projects of Henan Province (084100510002) to G.Z.

References

1. Bush, J. A.; Long, B. H.; Catino, J. J.; Bradner, W. T.; Tomita, K. *J. Antibiot.* **1987**, *40*, 668.
2. Kojiri, K.; Kondo, H.; Yoshinari, T.; Arakawa, H.; Nakajima, S. *J. Antibiot.* **1991**, *44*, 723.
3. Zhang, G.; Shen, J.; Cheng, H.; Zhu, L.; Fang, L.; Luo, S.; Muller, M. T.; Lee, G. E.; Wei, L.; Du, Y.; Sun, D.; Wang, P. G. *J. Med. Chem.* **2005**, *48*, 2600.
4. Curry, S.; Mandelkow, H.; Brick, P.; Franks, N. *Nat. Struct. Biol.* **1998**, *5*, 827.
5. Bhattacharya, A. A.; Grüne, T.; Curry, S. *J. Mol. Biol.* **2000**, *203*, 721.
6. He, X. M.; Carter, D. C. *Nature* **1992**, *358*, 209.
7. Kragh-Hansen, U. *Pharmacol. Rev.* **1981**, *33*, 17.
8. Carter, D. C.; Chang, B.; Ho, J. X.; Keeling, K.; Krishnasami, Z. *Eur. J. Biochem.* **1994**, *226*, 1049.
9. Guharay, J.; Sengupta, B.; Sengupta, P. K. *Proteins* **2001**, *43*, 75.
10. Perry, J. L.; Il'ichev, Y. V.; Kempf, V. R.; McClendon, J.; Park, G.; Manderville, R. A.; Rüker, F.; Dockal, M.; Simon, J. D. *J. Phys. Chem. B* **2003**, *107*, 6644.
11. Olson, R. E.; Christ, D. D. *Ann. Rep. Med. Chem.* **1996**, *31*, 327.
12. Lakowicz, J. R. *Principles of Fluorescence Spectroscopy*, 2nd ed.; Plenum Press: New York, 1999. pp 237–265.
13. Rubio, S.; Gomez-Hens, A.; Ualcarcel, M. *Talanta* **1986**, *33*, 633.
14. Li, D. J.; Zhu, J. F.; Jin, J.; Yao, X. J. *J. Mol. Struct.* **2007**, *846*, 34.
15. Hua, Y. J.; Liu, Y.; Wang, J. B.; Xiao, X. H.; Qu, S. S. *J. Pharm. Biomed. Anal.* **2004**, *36*, 915.
16. Cui, F. L.; Fan, J.; Fan, Y. C.; Li, W.; Hu, Z. D. *J. Pharm. Biomed. Anal.* **2004**, *34*, 189.
17. Faul, M. M.; Sullivan, K. A.; Grutsch, J. L.; Winneroski, L. L.; Shih, C.; Sanchez-Martinez, C.; Cooper, J. T. *Tetrahedron Lett.* **2004**, *45*, 1095.
18. Gerbanowski, A.; Malabat, C.; Rabiller, C.; Gueguen, J. *J. Agric. Food Chem.* **1999**, *47*, 5218.
19. Ahmad, B.; Parveen, S.; Khan, R. H. *Biomacromolecules* **2006**, *7*, 1350.
20. Eftink, M. R.; Ghiron, C. A. *Anal. Biochem.* **1981**, *114*, 199.
21. Lakowicz, J. R. *Principles of Fluorescence Spectroscopy*, 2nd ed.; Kluwer Academic/Plenum Publishers: New York, 1999.
22. Eftink, M. R. In *Biophysical and Biochemical Aspects of Fluorescence Spectroscopy*; Dewey, T. G., Ed.; Plenum: New York, 1991.
23. Ware, W. R. *J. Phys. Chem. A* **1962**, *66*, 455.
24. Scatchard, G. *Ann. NY Acad. Sci.* **1949**, *51*, 660.
25. Jiang, C. Q.; Gao, M. X.; Meng, X. Z. *Spectrochim. Acta, A: Mol. Biomol. Spectrosc.* **2003**, *59*, 1605.
26. Juziro, N.; Noriko, M. *Chem. Pharm. Bull.* **1985**, *33*, 2522.
27. Ross, P. D.; Subramanian, S. *Biochemistry* **1981**, *20*, 3096.
28. Sklar, L. A.; Hudson, B. S.; Simoni, R. D. *Biochemistry* **1977**, *16*, 5100.
29. Cui, F. L.; Fan, J.; Li, J. P.; Hu, Z. D. *Bioorg. Med. Chem.* **2004**, *12*, 151.
30. Berde, C. B.; Hudson, B. S.; Simoni, R. D.; Sklar, L. A. *J. Biol. Chem.* **1979**, *254*, 391.
31. Eftink, M. R. Fluorescence quenching reactions: probing biological macromolecular structures. In *Biophysical and Biochemical Aspects of Fluorescence Spectroscopy*; Dewey, T. G., Ed.; Plenum: New York, 1991; pp 105–133.
32. Peters, T. *Biochemistry, Genetics and Medical Applications*; Academic Press: San Diego, CA, 1996.
33. Steinhardt, J.; Krijn, J.; Leidy, J. G. *Biochemistry* **1971**, *10*, 4005.
34. Dockal, M.; Carter, D. C.; Rüker, F. *J. Biol. Chem.* **2000**, *275*, 3042.
35. Lloyd, J. B. F. *Nat. Phys. Sci.* **1971**, *231*, 64.
36. Lloyd, J. B. F. *J. Forensic Sci. Soc.* **1971**, *11*, 83.
37. Apicella, B.; Ciajolo, A.; Tregrossi, A. *Anal. Chem.* **2004**, *76*, 2138.
38. Kragh-Hansen, U.; Hellec, F.; de Foresta, B.; le Maire, M.; Møller, J. V. *Biophys. J.* **2001**, *80*, 2898.
39. Miller, J. N. *Anal. Proc.* **1979**, *16*, 203.